CROATICA CHEMICA ACTA CCACAA **65** (2) 237–267 (1992)

ISSN 0011-1643
UDC 541.1
CCA–2056 *Original Scientific Paper*

Simulation of the Kinetics of Aggregation: Fractals and Scaling

Paul Meakin

Department of Physics, University of Oslo,
P.O. Box 1048, Oslo 0316, Norway

Received June 26, 1991

In many processes of interest in physics, chemistry and biology small particles come together to form large structures. The fractal geometry of small particle aggregates plays an important role in their physical behavior including the kinetics of the aggregation process itself. The kinetics of aggregation can frequently be described by a mean field Smoluchowski equation. The geometric scaling properties (fractal geometry) of the aggregating clusters determine the scaling symmetry of the reaction kernel which in turn determines the asymptotic form of the cluster size distribution and the growth of the mean cluster size. In most simple systems, the asymptotic cluster size distribution can be described by the scaling form $N_s(t) \sim s^{-\theta} f(s/S(t))$ where $N_s(t)$ is the number of clusters of size s at time t and $S(t)$ is the mean cluster size at time t. This scaling form can be used in circumstances where the Smoluchowski equation does not provide an adequate representation of the aggregation kinetics.

INTRODUCTION

Processes in which particles join together to form larger structures called flocs or aggregates are important in many areas of science and technology. Because of their practical importance, these processes have been of considerable interest throughout this century. In recent years this interest has been stimulated by the role played by aggregation in processes such as air and water pollution, the nuclear winter scenario and the formation of ceramic materials with superior properties. In addition, the realization that structures formed by the aggregation of small particles can often be described quite successfully in terms of the concepts of fractal geometry[1] has generated a renewed theoretical interest in such phenomena. Much of the recent work of fractal aggregates was stimulated by the introduction of the diffusion-limited aggregation (DLA) model by Witten and Sander[2] in 1981. In this model particles are added, one at time, to a growing cluster or aggregate of particles *via* random walk trajectories starting from outside of the region occupied by the cluster. The structures generated in this way are random ramified clusters with a fractal dimensionality (D) substantially

smaller than the Euclidean dimensionality (d) of the embedding space or lattice. The DLA model is still of considerable interest; it represents a major theoretical challenge and provides a basis for understanding a broad range of phenomena including fluid-fluid displacement in porous media, dielectric breakdown processes, dissolution processes, random dendritic growth and some types of biological growth processes (see references 3–5 for reviews of these applications). However, the DLA model does not provide an adequate description of most colloidal aggregation processes. Meakin[6] and Kolb[7] simultaneously, but independently, developed a diffusion-limited cluster–cluster aggregation model that provides a quite realistic model for some fast aggregation processes, such as the flocculation of colloidal gold particles.[8] In this model particles and clusters move on a lattice *via* random walk trajectories. Whenever two objects (particles or clusters) contact each other, they are irreversibly combined and the combined cluster continues to move on the lattice. In most models the diffusion coefficient $\mathcal{D}(s)$ for clusters containing s particles or sites is assumed to be given by the algebraic relationship

$$\mathcal{D}(s) \sim s^{\gamma} \tag{1}$$

Figure 1 shows several stages in such a simulation. For negative values of the exponent γ in equation (1) the clusters generated by this model appear to be self-similar fractals with fractal dimensionalities of about 1.40–1.45 for $d = 2$ and 1.75–1.80 for $d = 3$. Theoretical considerations[9] and simulation results indicate that the fractal dimensionality, D, has a very weak dependence on γ in this regime.

Much earlier, Sutherland[10-12] developed a ballistic cluster–cluster aggregation model in which the particles and clusters follow linear (ballistic) trajectories. From large scale simulations in which the cluster velocities are assumed to be given by the kinetic theory of gases[13] a fractal dimensionality of about 1.95 is obtained.[14] This model describes quite well processes such as the aggregation of very small particles and clusters in flames and the aggregation of ceramic »nano-particles« in inert gases at reduced pressure. It is also believed to provide a basis for understanding the early stages of accretion in the primordial solar nebula.[1]

In the diffusion-limited and ballistic cluster–cluster aggregation models, the particles and clusters follow trajectories that have fractal dimensionalities (D_w) of 2 and 1, respectively. In the reaction limited aggregation process[15,16] the particles and clusters can be considered to follow zero dimensional trajectories. This model can be used to describe quite a wide variety of slow aggregation processes in dense fluids.[17] In these processes, a short range repulsive barrier must be overcome by thermal fluctuations before a pair of clusters can contact and become irreversibly joined. This process can be represented by a random selection of bonding (contacting) configurations between pairs of clusters with equal probabilities. The clusters generated by this model have fractal dimensionalities of about 1.55 for $d = 2$ and about 2.1 for $d = 3$. These simple aggregation models provide a surprisingly realistic description of a broad range of processes.

Although interest was initially focussed on the fractal structure of the clusters generated by these models, it was soon realized that they could also be used to explore the kinetics of aggregation processes.[18-21] In particular, it was found that the time dependent cluster size could be described by the simple scaling form[18]

$$N_s(t) \sim s^{-2} f(s/S(t)) \tag{2}$$

where $N_s(t)$ is the number of clusters of size s at time t and $S(t)$ is the »mean cluster size« given by

$$S(t) = \sum_{s=1}^{\infty} s^2 N_s(t) / \sum_{s=1}^{\infty} s N_s(t) \ . \tag{3}$$

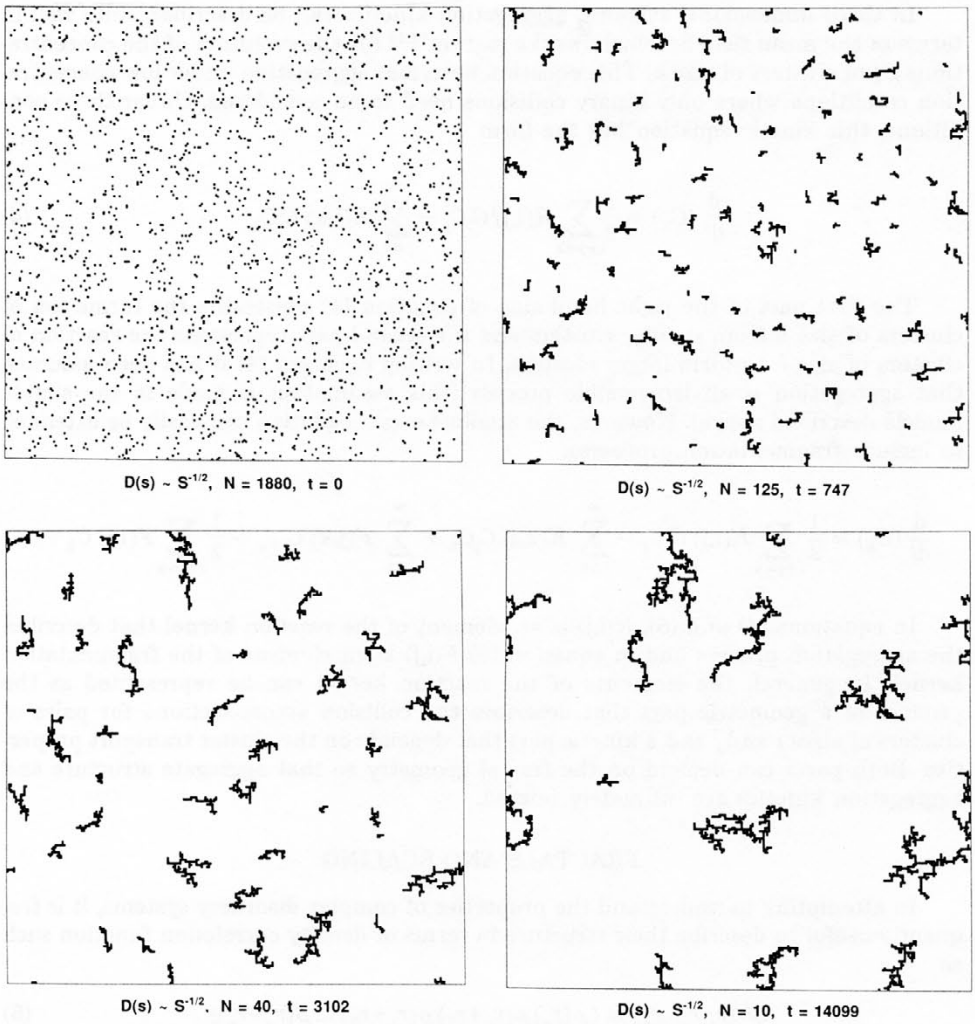

Figure 1. Four stages in a small scale simulation of diffusion-limited cluster–cluster aggregation on a square lattice with periodic boundary conditions. In this simulation, the cluster diffusion coefficients $\mathcal{D}(s)$ were assumed to be related to the cluster sizes (s) by $\mathcal{D}(s) \sim s^{-1/2}$. Figures 1a (upper left), 1b (upper right), 1c (lower left) and 1d (lower right) show the system in stages at which the total number of clusters N has reached a value of 1880, 125, 40 and 10, respectively. Figure 1a shows the initial stage after 2000 particles have been placed on randomly selected sites to form 1880 clusters.

Clusters generated by these models have also been used quite extensively to explore properties such as light scattering,[22-26] the aerodynamic[27] and hydrodynamic[28-35] behavior of fractal aggregates, mechanical properties,[36-41] diffusion on fractals[42-46] (fractons) *etc.*[47] Properties such as the aerodynamic and hydrodynamic transport coefficients must be understood in order to develop a theoretical description of the kinetics of aggregation.

In three dimensional systems, aggregation kinetics can be described quite well in terms of the mean field Smoluchowski equation[48,49] for the evolution of the concentrations C_k of clusters of size k. This equation describes aggregation under low concentration conditions where only binary collisions need to be considered. Under these conditions, this kinetic equation has the form

$$\frac{d}{dt}(C_k) = \frac{1}{2}\sum_{i+j=k} K(i,j)\, C_i C_j - \sum_{j=1}^{\infty} K(j,k)\, C_j C_k \,. \tag{4}$$

The first part of the right hand side of equation (4) represents the formation of clusters of size k from smaller clusters and the second part represents the reaction of clusters of size k to form larger clusters. In writing equation (4) it has been assumed that aggregation is an irreversible process (this assumption is made in the simple models described above). However, the Smoluchowski equation can easily be extended to include fragmentation processes.

$$\frac{d}{dt}(C_k) = \frac{1}{2}\sum_{i+j=k} K(i,j)\, C_i C_j - \sum_{j=1}^{\infty} K(k,j)\, C_j C_k + \sum_{j=1}^{\infty} F(j,k)\, C_{j+k} - \frac{1}{2}\sum_{i+j=k} F(i,j)\, C_k \,. \tag{5}$$

In equations (4) and (5), $K(i,j)$ is an element of the reaction kernel that describes the aggregation process and in equation (5) $F(i,j)$ is an element of the fragmentation kernel. In general, the elements of the reaction kernel can be represented as the product of a geometric part that describes the collision »cross-section« for pairs of clusters of sizes i and j and a kinetic part that depends on the cluster transport properties. Both parts can depend on the fractal geometry so that aggregate structure and aggregation kinetics are intimately related.

FRACTALS AND SCALING

In attempting to understand the properties of complex disordery systems, it is frequently useful to describe their structure in terms of density correlation function such as

$$C^n(r_1, r_2 \ldots r_n) = \langle \rho(r_o)\, \rho(r_o + r_1)\, \rho(r_o + r_2) \ldots \rho(r_o + r_n) \rangle \,. \tag{6}$$

Here, $\rho(r)$ is the density at position r and the product of densities on the right hand size of equation (6) is averaged over all origins (r_o) in the structure. For a self-similar homogeneous fractal the correlation function $C^n(r_1, r_2 \cdots r_n)$ is a homogeneous function of its arguments.

$$C^n(\lambda r_1, \lambda r_2 \ldots \lambda r_n) = \lambda^{-n\alpha}[C^n(r_1, r_2 \ldots r_n)] \tag{7}$$

where the exponent α in equation (7) is the codimensionality ($\alpha = d - D$) of the fractal. In practice, the most commonly used density correlation function is the two point density–density correlation function

$$C(r) = \langle\langle \rho(r_o)\rho(r_o+r)\rangle\rangle_{|r|=r} \tag{8}$$

Here, the correlation function has been averaged over all origins in the cluster and all orientations. This quantity is important in practice since it determines the scattering properties of the cluster (small angle single scattering) and is commonly used to measure the fractal dimensionality of real systems (from digitized images) and computer-generated structures.

Equation (7) implies that the two point density–density correlation function has the algebraic form

$$C(r) \sim r^{-\alpha} \tag{9}$$

For real structures, this power law behavior extends over only a limited range of length scales and in practice it can be quite difficult to obtain a reliable estimate of α (and consequently the corresponding fractal dimensionality $D_\alpha = d-\alpha$) from the dependence of log ($C(r)$) on log (r).

For structures of finite size the two point density–density correlation function will depend on the overall size of the structure described by a characteristic length R as well as the internal length r. In this case, the correlation function can be written as $C(r,R)$. The function $C(r,R)$ represents the density–density correlation function averaged over a large number of structures of the same size or characteristic length R. If large clusters are (on average) related to small clusters by a change of length scale, it is natural to assume that $C(r,R)$ is a homogeneous function of its arguments so that

$$C(\lambda r, \lambda R) = \lambda^{-\alpha} C(r,R) \tag{10}$$

Taking a value of $1/R$ for λ, we have

$$C(r/R,1) = R^{\alpha} C(r,R) \tag{11}$$

or

$$C(r,R) = R^{-\alpha} f(r/R) \tag{12}$$

According to this scaling assumption, the density–density correlation function for systems of different sizes (R) can be expressed in terms of the scaling form given in equation (12). The function $f(x)$ is called the scaling function and the exponent α is a scaling exponent. If equation (12) provides a valid description of the geometric scaling properties, then plots of $R^{\alpha}C(r,R)$ *vs.* r/R for structures of different sizes will fall on a common curve (the scaling function $f(x)$). This is illustrated for clusters generated using a three dimensional off-lattice model for diffusion limited cluster–cluster aggregation in Figure 2. Figure 2a shows the two point density–density correlation functions for clusters of five different sizes (100, 300, 1000, 3000 and 10,000 particles). In this case, it is more convenient to select clusters of a particular size (number of particles, s), rather than a particular value (or small range of values), of the characteristic length R. Since s and R are related by

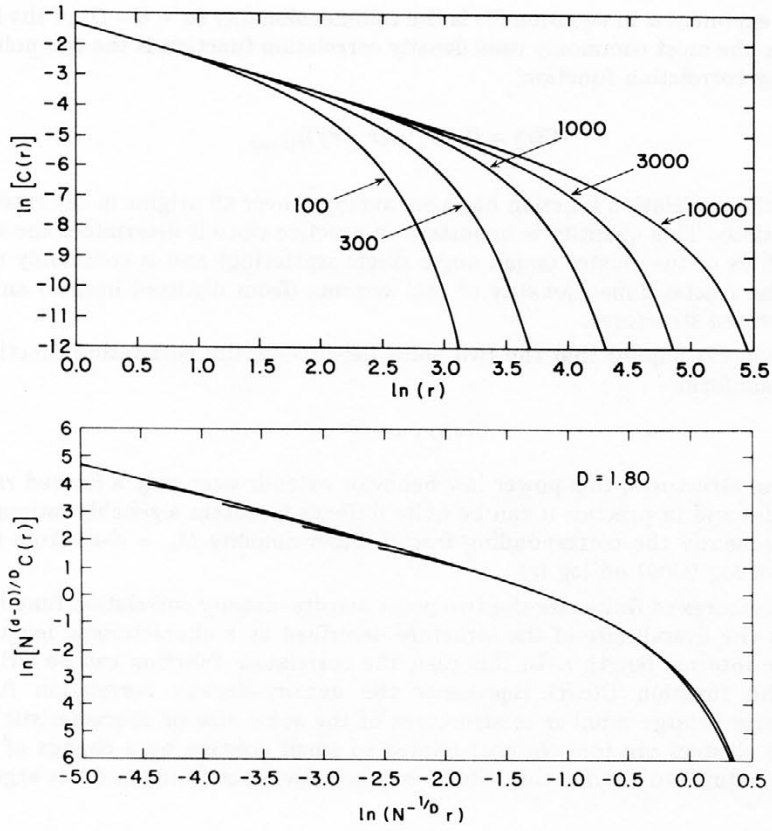

Figure 2. Scaling of the two point density-density correlation function for clusters generated using an off-lattice diffusion-limited cluster–cluster aggregation model. Figure 2a (top) shows the correlation functions obtained from 10,000 100 particle clusters, 1000 300 particles clusters, 100 1000 particle clusters, 39 3000 particle clusters and 13 10,000 particle clusters. Figure 2b (bottom) shows how these correlation functions can be scaled onto a common curve using the scaling form given in equation (15).

$$\langle R \rangle \sim s^{-1/D} \tag{13}$$

for fractal objects equation (12) can be written as

$$C(r,s) = s^{-\alpha/D} f(r/s^{1/D}) \tag{14}$$

and since the exponent α in equation (14) is the codimensionality, we have

$$C(r) = s^{(D-d)/D} f(r/s^{1/D}) \ . \tag{15}$$

In Figure 2b plots of ln $[s^{(d-D)/D} C(r)]$ *vs.* ln $(s^{-1/D} r)$ are shown for the five different cluster sizes. The fact that these curves overlap almost perfectly confirms the simple

scaling assumption. This shows that both the internal density correlations and the global scaling properties of the cluster (such as the dependence of the radius of gyration on its mass) can be described in terms of the same fractal dimensionality.

It has been known for some time that for a variety of systems the cluster size distribution evolves towards a »self preserving« form that is independent of the initial cluster size distribution.[50-53] This observation motivates a scaling description of the time dependent cluster size distribution. Here, we assume that the cluster size distribution can be presented as a homogeneous function of the cluster sizes (s) and the »mean« cluster size (S). In most cases, S is defined according to equation (3). It is possible to use other moment ratios of the cluster size to define different characteristic cluster sizes but care must be taken if the cluster size distribution is broad. It follows from the homogeneity assumption that the cluster size distribution can be represented by the scaling form

$$N_s(t) \sim s^{-\theta} \, \mathrm{f}(s/S(t)) \ . \tag{16}$$

In mass conserving systems, the exponent θ has a value of 2.0. This can be demonstrated by writing the total mass (total number of particles) as

$$M = \sum_{s=1}^{\infty} s \, s^{-\theta} \, \mathrm{f}(s/S(t)) \tag{17}$$

in the asymptotic limit (late time and large cluster sizes), the summation in equation (17) can be replaced by an integration

$$M = \int_0^{\infty} s^{1-\theta} \, f(s/S(t)) \, \mathrm{d}s \tag{18}$$

and making the substitution $x = s/S(t)$ we have

$$M = S(t)^{2-\theta} \int_0^{\infty} x^{1-\theta} \, f(x) \, \mathrm{d}x \tag{19}$$

Since the integral has a constant value and M is constant, it follows that θ must have a value of 2 so that the cluster size distribution can be represented by the scaling form given in equation (2).

This scaling form[18-20] has been applied successfully to a very wide range of aggregating systems involving fractal and non-fractal objects. It is said to be a »super-universal« scaling form since it applies equally well to systems in embedding spaces with different dimensionalities. The simple scaling behavior associated with these aggregation processes reflects underlying symmetries in the kinetic equations that describe the aggregation processes. These in turn are a consequence of the geometric scaling properties associated with the structures of the aggregation clusters.

There are no characteristic length scales associated with the internal structure of fractal objects. In simple aggregating systems there are generally two characteristic length scales (apart from that associated with the particle size). One is associated with

the mean cluster size and the other is associated with the mean distance separating these clusters. The kinetics of simple aggregation processes can often be understood in terms of these lengths, which are closely related to each other. For example, in a mass conserving systems in which the cluster size distribution is not too broad the characteristic length (R_s) associated with the clusters is given by

$$R_s \sim S^{1/D} \tag{20}$$

and the number of clusters N is given by

$$N \sim S^{-1} \tag{21}$$

This means that the characteristic length (R_d) separating the clusters is given by

$$R_d \sim N^{-1/d} \sim S^{-1/d} \sim R_s^{D/d} . \tag{22}$$

In general, for a system with two characteristic length scales, both lengths would appear in the scaling form describing the evolution of the system. However, since R_s and R_d are related by a simple homogeneous power law (equation (22)) it is necessary to use only a single length (R_d or R_s) or the characteristic cluster size S that is related to both of them by simple power laws.

In many systems, the mean cluster size $S(t)$ grows algebraically

$$S(t) \sim t^z \tag{23}$$

in the limit $t \to \infty$ so that equation (2) can be replaced by

$$N_s(t) \sim s^{-2} f'(s/t^z) . \tag{24}$$

It is also often convenient to express time dependent size distribution in terms of the scaling form[21]

$$N_s(t) \sim s^{-\tau} t^{-\omega} g(s/t^z) \tag{25}$$

Here, the cluster size dependence and the time dependence of $N_s(t)$ for small values of s/t^z has been expressed explicitly in the first two terms on the right hand side of equation (25). The function $g(x)$ in equation (25) has the form $g(x) = \text{const.}$ for $x \ll 1$ and $g(x)$ decreases faster than any power of x for $x \gg 1$. The scaling forms given in equations (24) and (25) are equivalent. This may be demonstrated by using equation (25) to calculate the total mass (M) of all of the clusters.

$$M = \sum_{s=1}^{\infty} s\, N_s(t) = \sum_{s=1}^{\infty} s^{1-\tau} t^{-\omega} g(s/t^z) . \tag{26}$$

In the asymptotic limit, the sum on the right hand side of equation (26) can be replaced by an integral

$$M = \int_0^\infty s^{1-\tau} t^{-\omega} g(s/t^z)\, ds \tag{27}$$

and making the substitution $x = s/t^z$, we have

$$M = t^{[(1-\tau)z - \omega + z]} \int_0^\infty x^{1-\tau} g(x)\, dx \ . \tag{28}$$

Since the total mass is conserved and the integral also has a constant value, equation (28) implies the scaling relationship

$$(2-\tau)z = \omega \ . \tag{29}$$

If the cluster size distribution is not a power law, then equation (25) can be replaced by

$$N_s(t) \sim t^{-\omega}\, g(s/t^z) \tag{30}$$

so that the exponent relationship

$$2z = \omega \tag{31}$$

is obtained. Substituting equation (29) in equation (25) gives

$$N_s(t) = s^{-\tau} t^{(2-\tau)z}\, g(s/t^z) \tag{32}$$

and replacing $g(x)$ by $x^{\tau-2}\, g'(x)$ we have

$$N_s(t) = s^{-\tau} t^{(2-\tau)z}\, s^{\tau-2} t^{(2-\tau)z}\, g'(s/t^z) \tag{33}$$

or

$$N_s(t) \sim s^{-2}\, g'(s/t^z) \ . \tag{34}$$

Similarly, the scaling form in equation (24) can also be recovered by substituting equation (31) into equation (30).

CLUSTER–CLUSTER AGGREGATION MODELS

Cluster–cluster aggregation models have been used extensively to study the structure of small particle aggregates and the kinetics of aggregations. The most simple model differ primarily in the nature (fractal dimensionality) of the trajectories used to bring clusters together. In this section, these model are described and the application to aggregation kinetics is illustrated.

Diffusion-Limited Cluster–Cluster Aggregation

In the diffusion-limited cluster–cluster aggregation model[6,7,54-56] particles and clusters are moved in a d dimensional space *via* random walk trajectories ($D_w = 2$). Whenever two (or more) objects (particles or clusters) contact each other, they are combined irreversibly in the contacting configuration to form a larger structure that

continues to move as a rigid entity. In most cases simple lattice models in which the clusters move by a single lattice unit in a randomly selected direction have been used to explore the kinetics of diffusion-limited cluster–cluster aggregation. In a typical simulation, a fraction ρ of the sites on the lattice (*i.e.*, a total of ρL^d sites) are selected at random and filled to represent the aggregating particles. Sites that are connected *via* nearest neighbor occupancy are identified as belonging to the same cluster and all of the clusters (including single particle clusters) are labelled. If ρ is sufficiently small, the system will contain mainly single particle clusters with a small number of small clusters. The aggregation process is represented by selecting clusters at random and moving them by one lattice unit in a randomly selected direction if $x < \mathcal{D}(s)/\mathcal{D}_{max}$. Here, x is a random number uniformly distributed over the range $0 < x < 1$ and $\mathcal{D}_{max}$ is the maximum diffusion coefficient for any of the clusters in the system. After each cluster has been selected, the time is incremented by an amount δt given by

$$\delta t = 1/(N\mathcal{D}_{max}) \tag{35}$$

where N is the total number of clusters. In most cases, the cluster diffusion coefficients, $\mathcal{D}(s)$, are assumed to be related to the cluster size, s, by the algebraic relationship given in equation (1). Each time a cluster is moved, its perimeter is examined for contact with other clusters and if contact is found, the contacting clusters are joined to form a larger cluster. This model leads to the formation of clusters that have a self-similar fractal structure ($D \approx 1.45$ for $d = 2$, $D \approx 1.80$ for $d = 3$, *etc.*) on length scales up to a correlation length ξ determined by the system density (ρ). The two point density–density correlation function at the end of a simulation when all the particles belong to a single cluster has the form

$$C(r) \sim r^{-\alpha} \qquad \text{for } r << \xi \tag{36}$$

$$C(r) = \rho \qquad \text{for } r >> \xi \tag{37}$$

the correlation length ξ is given by

$$\xi \sim \rho^{-1/\alpha} \tag{38}$$

and the correlation function can be written as

$$C(r) \sim r^{-\alpha} f(r/\xi) \tag{39}$$

where the function $f(x)$ has the form $f(x) = \text{const.}$ $(x <<)$ and $f(x) \sim x^{\alpha}$ for $x >> 1$. If the density is sufficiently small, the correlation length ξ will exceed the characteristic length associated with the mean cluster size (R_s) throughout all or most of the simulation. These considerations indicate that for a simulation carried out using 10,000 sites (particles) on a $128 \times 128 \times 128$ site lattice ($\rho \sim 5 \times 10^{-3}$) the correlation length (ξ) will be approximately equal to the system size (L) so that the aggregation kinetics will be essentially unaffected by both finite size and non-zero density effects until quite late stages in the simulated aggregation process.

If the cluster size distribution is sufficiently narrow, the kinetics of the aggregation process can be determined by course graining the system into regions of size R_s where

R_s is the characteristic cluster size. The evolution of the number of clusters $N(t)$ is then given by

$$dN/dt \sim -N S^{\gamma} S^{-2/D} S^{(d/D-1)} . \tag{40}$$

The term $S^{\gamma}S^{-2/D}$ in the right hand side of equation (40) represents the time required by a typical cluster to move a distance R_s and the term $S^{(d/D-1)}$ is the probability that it will encounter another cluster after moving a distance R_s. Since $N(t)$ and $S(t)$ are related by

$$S(t) \sim N(t)^{-1} \tag{41}$$

equation (40) becomes

$$\frac{dN}{dt} \sim -N^{(2/D - \gamma + 1 - d/D)} \tag{42}$$

from which we obtain the result

$$N(t) \sim t^{-z'} \tag{43}$$

where the exponent z' is given by

$$z' = \frac{1}{1 - (2 - d - \gamma D)/D} \tag{44a}$$

or

$$z' = \frac{D}{D + 2 - \gamma D - d} . \tag{44b}$$

Simple scaling arguments and more detailed considerations (see below) indicate that the diffusion coefficient for a fractal cluster moving through a quiescent fluid is given by

$$\mathcal{D}(s) \sim s^{-1/D} \tag{45}$$

(*i.e.*, $\gamma = -1/D$) substituting this value for γ and $d = 3$ in equation (44) indicates that the exponent z' in equation (43) has a value of 1. Similarly, the exponent z describing the growth of the mean cluster size

$$S(t) \sim t^{z} \tag{46}$$

also has a value of 1. Figure 3 shows the cluster size distribution obtained from simulations carried out using a three dimensional (cubic lattice) diffusion-limited cluster–cluster aggregation model in which equation (45) was assumed to describe the size dependence of the cluster diffusion coefficients. In Figure 3b, these cluster size distributions have been scaled using the scaling form

$$N_s(t) \sim s^{-2} f(s/t^{z}) \tag{47}$$

since $S(t)$ is related to the time t by equation (46), this scaling form is asymptotically equivalent to that given in equation (2). Figure 3b shows that a reasonably good data

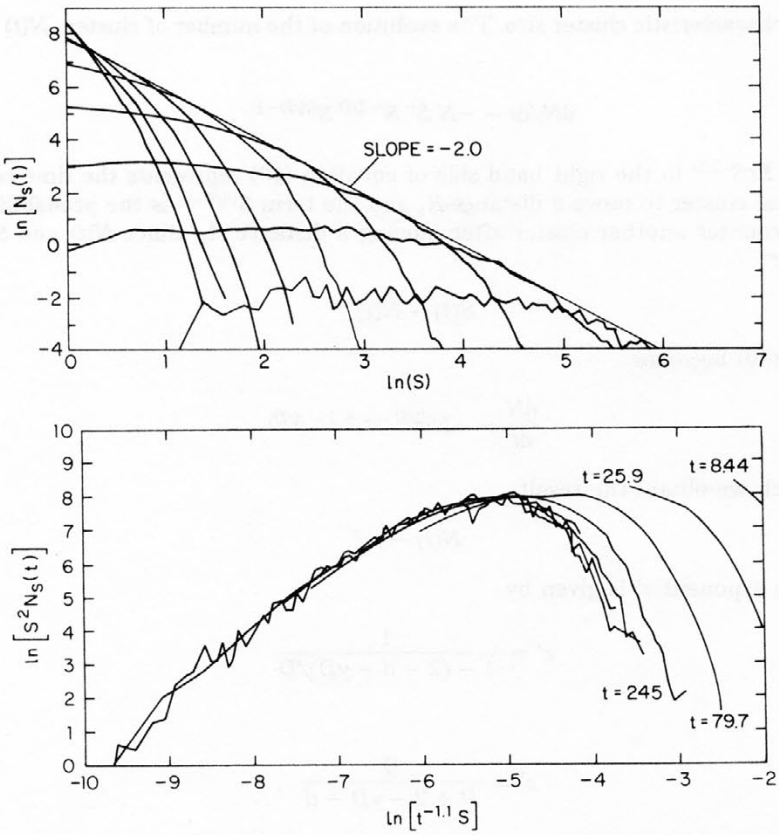

Figure 3. Cluster size distributions ($N_s(t)$) obtained at 9 stages (times) during simulations of diffusion-limited cluster–cluster aggregation on a cubic lattice with cluster diffusion coefficients given by $O(s) \sim s^{-1/D}$. Figure 3a (top) shows the size distributions and Figure 3b (bottom) shows the results of an attempt to scale these distributions using the scaling form given in equation (47). The data collapse is quite good at late times but at early times (t = 8.44, 25.9 and 79.7) the cluster size distributions cannot be scaled.

collapse is obtained using a value for the exponent z in equation (47) that is quite close to 1.0. Direct measurement on the exponents z and z' from the time dependence of $S(t)$ and $N(t)$ give values for z and z' that are also close to 1.0. The deviation of the effective value of z from the theoretical value is attributed to finite size and non-zero concentration effects. The scaling form given in equation (2) is more convenient and, in at least some cases, gives a better data collapse than that given in equation (47). In general, scaling is only expected to work in the large time, large cluster size asymptotic limit. Figure 3 shows quite clearly that the cluster size distributions at early times cannot be described in terms of the scaling form given in equation (47).

In writing equation (40) to describe the rate of collision between pairs of clusters it was assumed that each time a cluster visits a new region of size R_s it has the same probability of finding a second cluster. This is a mean field assumption that breaks

down for lower dimensional systems. For the case $d = 3$, equation (40) appears to provide a satisfactory description of the overall aggregation kinetics. However, for $d = 2$, equation (40) must be modified and the mean field description breaks down completely for $d<2$. In a two dimensional system, the asymptotic dependence of the number of new regions (for example the number of sites in an on-lattice random walk) visited by random walkers after N steps is given by

$$N_f = N/\log(N) \tag{48}$$

Since the relative trajectory followed by pairs of clusters in a diffusion-limited cluster–cluster aggregation process is also a random walk, equation (40) must be modified for aggregation on a two dimensional substrate. For $D = d$, the aggregating system at time t_2 can be rescaled onto a system at time t_1 by changing the length scale of the system by a factor λ given by

$$\lambda = [S(t_2)/S(t_1)]^{1/D} \tag{49}$$

In the asymptotic regime, the fraction of space »occupied« by the clusters does not change and equation (40) can still be used.

If $D<d$ (as it is in the case in cluster–cluster aggregation) the aggregation process is accelerated because the fraction of the space that is occupied by the clusters increases with increasing cluster size. Under these conditions, the »asymptotic« growth of the mean cluster size and decay of the number of clusters are given by[57]

$$S(t) \sim [t \ln(t)]^{z} \tag{50a}$$

and

$$N(t) \sim [t \ln(t)]^{-z'} \tag{50b}$$

where $z = z'$ and z' is given by equation (44). Eventually, the fraction of space »occupied« by the clusters will become large, equation (50) will break down and, in an infinite system, a cluster of infinite size will appear in a finite time (*i.e.*, gellation will occur). If $D>d$ (as it is in the diffusion-limited particle coalescence model[58] in which contacting particles are combined into a single particle or site with mass conservation), the particles or aggregates occupy a smaller and smaller fraction of the system as the number of objects in the system decreases. This contributes to a slowing down of the processes, which is further augmented by the inefficiency of the two dimensional random walk in exploring »new space«. In this case, the asymptotic result

$$N(t) \sim [t/\ln(t)]^{-z'} \tag{51a}$$

$$S(t) \sim [t/\ln(t)]^{z} \tag{51b}$$

is obtained.

Figure 4 shows the results from a two dimensional diffusion-limited cluster–cluster aggregation model carried out with a diffusion coefficient exponent γ (equation 1) of -1. Figure 4a shows the dependence of N and S on $t \ln(t)$. These results support the idea that the growth of the mean cluster size is described by

$$S(t) \sim t \ln(t)^{z} \tag{52}$$

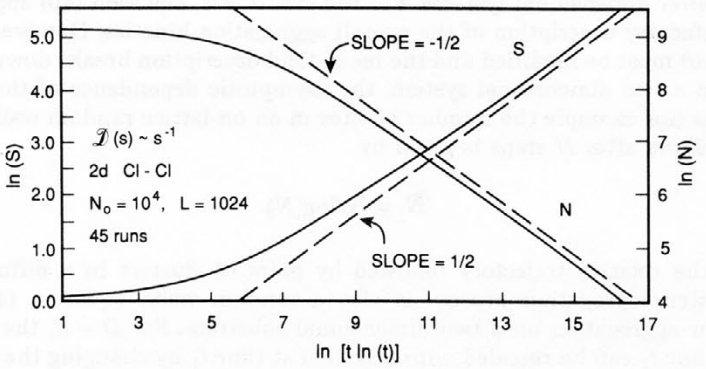

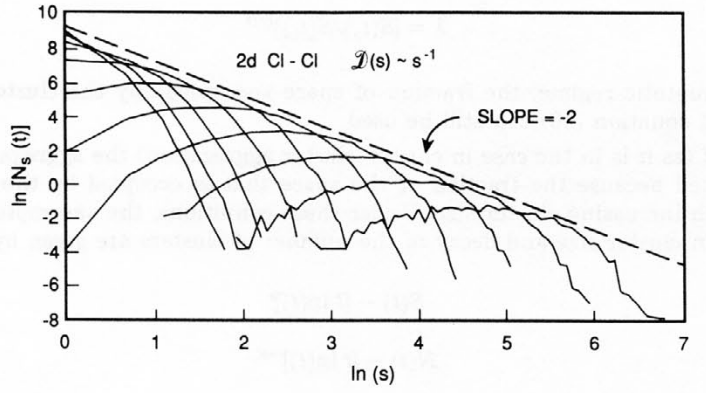

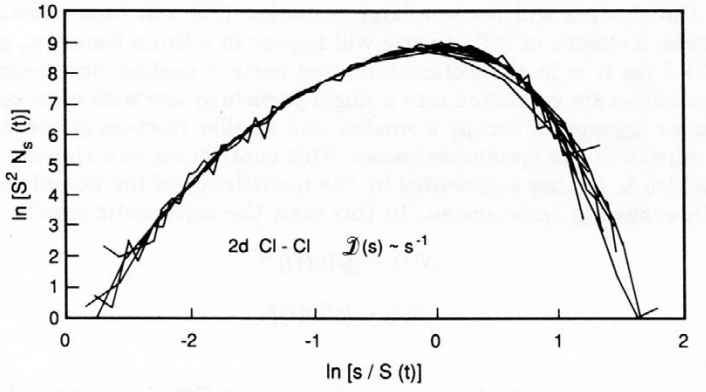

Figure 4. Results obtained from a two dimensional diffusion-limited cluster–cluster aggregation model. Figure 4a (top) shows the algebraic growth of $S(t)$ and the decay of $N(t)$. Figure 4b (middle) shows the cluster size distribution at ten different stages (times) and Figure 4c (bottom) shows how these distributions can be scaled using the scaling form given in equation (2). In these simulations, cluster diffusion coefficients $D(s)$ are proportional to s^{-1}.

where z is given by equation (42) and that the decrease in the number of clusters is given by equation (51a). Figure 4b shows the time dependent cluster size distributions $N_s(t)$ from the same simulations and Figure 4c shows quite a good data collapse obtained using the scaling form given in equation (2).

The kinetics of three dimensional diffusion-limited cluster–cluster aggregation can be described in terms of a Smoluchowski equation. In the low density limit, only binary collisions need be considered. Since $2D+D_w>d$ (2x1.8+2>3 for the three dimensional case), a pair of clusters following random walk trajectories behave like impenetrable spheres with radii $r(s)$ given by $r(s) \sim s^{1/D}$. Consequently, the collision between a pair of clusters of sizes s_1 and s_2 can be represented by the absorption of a particle on a stationary surface of radius $R(s_1,s_2) \sim s_1^{1/D} + s_2^{1/D}$. The diffusion coefficient of the particle with respect to the stationary surface is given by

$$\mathcal{D}(s_1,s_2) \sim s_1^{-1/D} + s_2^{-1/D} \tag{53}$$

and the element $K(s_1,s_2)$ of the reaction kernel for clusters of size s_1 and s_2 is given by

$$K(s_1,s_2) \sim (s_1^{1/D} + s_2^{1/D})^{d-2} (s_1^{-1/D} + s_2^{-1/D}) \tag{54}$$

The first term on the right hand side of equation (54) is a geometric term that depends on the cluster structures and the shape of their relative trajectories. The second term depends on the transport properties of the clusters. For the case $d = 3$, equation (54) becomes

$$K(s_1,s_2) \sim (s_1^{1/D} + s_2^{1/D}) (s_1^{-1/D} + s_2^{-1/D}) \tag{55}$$

The elements of this reaction kernel have an almost constant value (independent of s_1 and s_2). However, the aggregation of large clusters with small clusters is favored and this is responsible for the depletion of very small clusters at long times seen in both simulations (Figure 3) and experiments. In simulations, the diffusion coefficient exponent γ need not be confined to an asymptotic value of $-1/D$ and the three dimensional reaction kernel has the form

$$K(s_1,s_2) \sim (s_1^{1/D} + s_2^{1/D}) (s_1^{\gamma} + s_2^{\gamma}) \tag{56}$$

This form for the reaction kernel has been confirmed by direct measurements of the rate of aggregation of clusters of different sizes in diffusion-limited cluster–cluster aggregation model simulations.[59]

Ballistic Cluster–Cluster Aggregation

The ballistic cluster–cluster aggregation process can be simulated by taking advantage of the fact that the »reaction kernel« can be written in the form

$$K(i,j) \sim \sigma(i,j)[(s_i + s_j)/s_i s_j]^{1/2} \ . \tag{57}$$

The first term on the right hand side of equation (57) represents the collision cross section for clusters i and j and the second term is obtained by assuming that the

cluster velocity distributions can be described in terms of the kinetic theory of gases[13] (*i.e.*, the clusters act like giant gas molecules). The model can easily be modified to include other velocity distributions by rewriting equation (57) as

$$K(i,j) \sim \sigma(i,j) \cdot V(s_i,s_j) \tag{58}$$

where $V(s_i, s_j)$ is obtained from the cluster velocity distribution. An upper limit for the collision cross-section is given by

$$Q(i,j) = \pi(R_i^m + R_j^m)^2 \tag{59}$$

where R_i^m and R_j^m are the maximum radii for clusters i and j.

In the ballistic cluster–cluster aggregation, model pairs of clusters are selected randomly from a list of clusters. An upper limit for the reaction probability for the pair of clusters is obtained from the expression

$$P(i,j) \sim (R_i^m + R_j^m)^2 \, [(s_i + s_j)/s_i s_j]^{1/2} \; . \tag{60}$$

A random number x $(0<x<1)$ is then generated and the clusters are returned to the list if

$$x > P(i,j)/P_{max} \tag{61}$$

where P_{max} is the maximum value of $P(i,j)$ for any pair of clusters in the system. If the randomly selected clusters are not rejected, they are rotated to random orientations and one cluster is »fired« at the other along a linear trajectory with a center to center impact parameter randomly selected from a circle of radius $(R_i^m + R_j^m)$. If this brings the clusters into contact with each other, they are combined irreversibly in their initial contact configuration to form a rigid cluster that is returned to the list of clusters. If they do not contact, the two clusters are returned to the cluster list. The process described above is repeated with other randomly selected cluster pairs until a pre-selected maximum cluster size or mean cluster size is reached.

The fractal dimensionality of clusters generated using this model is approximately 1.95.[14,60] The reaction kernel for this model can be obtained based on the idea that two fractals with a dimensionality of 1.95 following a relative trajectory with a dimensionality of $D_w = 1.0$ cannot interpenetrate each other. This means that clusters of similar sizes (s_i and s_j) will have a mutual cross-section given by

$$\sigma(i,j) \approx (s_i^{1/D} + s_j^{1/D})^2 \; . \tag{62}$$

For clusters of much different sizes $(s_i > s_j)$, we can make use of the fact that for $D<2$ the projection of a cluster onto a plane has a fractal dimensionality of D. The collision cross-section for the two clusters can then be obtained by projecting them onto the same plane (perpendicular to the trajectory). The collision cross-section is then given by

$$\sigma(i,j) \sim \sigma(s_j,s_j) \cdot N(s_j^{1/D},i) \tag{63}$$

where $\sigma(s_i s_j)$ is the collision cross-section for two clusters of size s_j and $N(s_j^{1/D},i)$ is the number of regions of size (linear spatial extent) $s_j^{1/D}$ needed to cover a fractal (prefractal) of size i. Since $\sigma(s_j,s_j) - s_j^{2/D}$ and $N(s_j^{1/D},i)$ is proportional to $s_i \cdot (s_j^{1/D})^{-D}$, we find that

$$\sigma(i,j) \approx s_i\, s_j^{2/D-1} \tag{64}$$

for the case $s_i \gg s_j$. From equations (62) and (64) we can conclude that equation (64) describes the asymptotic (large cluster) size collision cross-section in both the $i \approx j$ and $i \gg j$ regimes. The complete reaction kernel for ballistic cluster–cluster aggregation may consequently be written as

$$K(i,j) \approx s_i\, s_j^{2/D-1}[(s_i + s_j)/s_i s_j]^{1/2} \qquad (i \geq j) \tag{65}$$

or

$$K(i,j) \approx s_i\, s_j^{(2/D-3/2)} \qquad (i \geq j) \tag{66}$$

The scaling of the diagonal elements of the reaction kernel can be written as

$$K(i,i) \sim i^{\lambda} \tag{67}$$

with

$$\lambda = 2/D - 1/2 \tag{68}$$

Figure 5 shows time dependent cluster size distribution obtained from simulations carried out using the ballistic cluster–cluster aggregation model. The cluster size distribution is quite broad but small clusters are eventually depleted and a characteristic cluster size emerges. At later times, these size distributions can be scaled quite well using the scaling form given in equation (2).

Using arguments similar to those discussed above for the diffusion-limited cluster–cluster aggregation model, we expect to find that the mean cluster size grows algebrai-

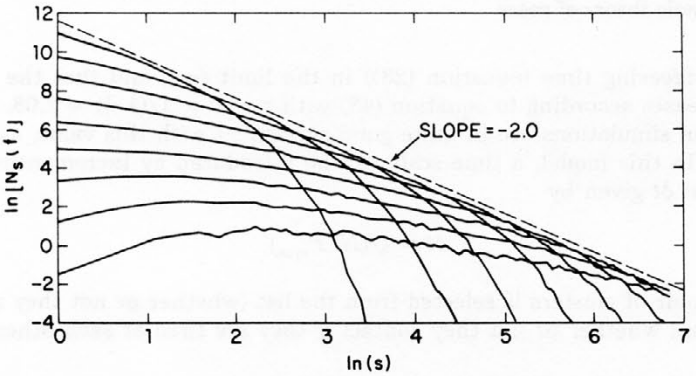

Figure 5. Cluster size distributions obtained from three dimensional off-lattice ballistic cluster–cluster aggregation model simulations in which the cluster velocity distributions were assumed to be given by the kinetic theory of gases. The size distributions ($N_s(t)$) at 9 stages obtained from 32 simulations each of which employed 200,000 particles are shown.

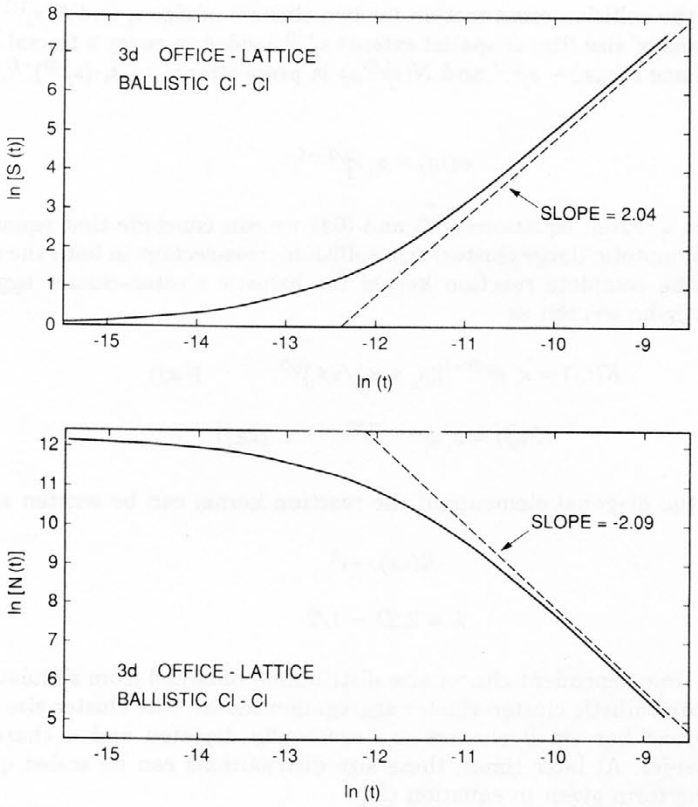

Figure 6. Time dependence of the mean cluster site (Figure 6a, top) and number of clusters (Figure 6b, bottom) obtained from the three-dimensional off-lattice ballistic cluster–cluster aggregation simulations. In these simulations, the cluster velocity distributions were assumed to be given by the kinetic theory of gases.

cally with increasing time (equation (23)) in the limit $t \to \infty$ and that the number of clusters decreases according to equation (43) with $z = z' = 1/(1-\lambda) \approx 2.08$. The values obtained from simulations are in quite good agreement with this value, as illustrated in Figure 6. In this model, a time scale can be introduced by incrementing the time by an amount δt given by

$$\delta t = 1/(N^2 P_{max}) \tag{69}$$

each time a pair of clusters is selected from the list (whether or not they are fired at each other and whether or not they contact if they are fired at each other).

Reaction-Limited Cluster–Cluster Aggregation

In reaction-limited cluster–cluster aggregation, many encounters between pairs of clusters are required before aggregation occurs. In the most simple aggregation models considered here it is assumed that once bonding has been established the clusters are

rigidly and irreversibly bound together. In some respects, the reaction-limited aggregation model is simpler than the ballistic and diffusion-limited aggregation models but it was developed more recently. The most simple reaction-limited cluster–cluster aggregation models are based on the idea that if the repulsive barrier that must be crossed to bring two clusters into contact with each other is sufficiently large (*i.e.*, if the sticking probability, σ, is sufficiently small), then the system will test a representative sample of all possible bonding configurations between pairs of clusters before selecting one of them at random. In this limit, the simulation reduces to the random selection of bonding configurations from all possible bonding configurations between pairs of clusters in the system.

An alternative approach to the simulation of reaction limited cluster–cluster aggregation is to use a diffusion-limited cluster–cluster aggregation model but join clusters together irreversibly with a small probability (σ') each time they attempt to overlap. In practice, it is only possible to reduce σ' to values of 10^{-3} to 10^{-4} in reasonably large scale simulation.[61] However, this allows us to approach reasonably close to the reaction limited ($\sigma' \to 0$) limit.

A hierarchical model for reaction-limited cluster–cluster[15,16] aggregation was developed by Jullien and Kolb.[15,16] In this model, 2^m particles are combined in stages so that at each stage the clusters are all of the same size. In this lattice model, all possible ways of joining pairs of clusters are found and one of these is selected at random. From simulations in which clusters containing up to 512 occupied sites were generated, effective dimensionalities of 1.53 ± 0.04, 1.98 ± 0.04 and 2.32 ± 0.04 were obtained for $d = 2$, 3 and 4.

Jullien and Kolb also measured the number of contacting configurations C_s for pairs of clusters containing s particles. They found that C_s depended algebraically on s according to $C_s \sim s^{\lambda'}$, where the exponent λ' had values of 0.74, 1.16 and 1.44 for $d = 2$, 3 and 4, respectively.

Brown and Ball[62] developed a model in which pairs of clusters are selected and placed at random on a cubic lattice. In this model, the selected pairs of clusters are combined only if they are adjacent to each other but do not overlap. Depending on how the clusters are selected, the cluster size distribution may be monodisperse (as it is the case in a hierarchical model) or may evolve in a natural way into a polydisperse cluster size distribution if the clusters are selected at random (irrespective of their sizes). Using this model, a fractal dimensionality of 1.94 ± 0.02 was found for the monodisperse case and 2.11 ± 0.03 for the polydisperse case in three-dimensional simulations. For $d = 2$, values of 1.53 ± 0.01 and 1.59 ± 0.01, respectively, were obtained. The exponent λ' was found to have values of 1.16 ± 0.04 and 1.06 ± 0.02 for the monodisperse and polydisperse three-dimensional model and 0.75 ± 0.01 and 0.73 ± 0.02 for the monodisperse and polydisperse two-dimensional models.

A reaction-limited aggregation model proposed by Leyvraz,[63] which is very closely related to the model of Brown and Ball,[62] has been investigated by Meakin and Family.[61,64] This model starts with a large number (N_0) of single particles. As the simulation proceeds, a pair of particles is selected randomly and placed in contact with each other. If the particles are contained in the same cluster, a new selection is made. If the particles are contained in different clusters, all the particles in theses clusters are moved with the selected pair of particles when they are moved into contact with each other. If the two clusters overlap, a new pair of particles is randomly selected. If no overlap is found, the two clusters are combined irreversibly.

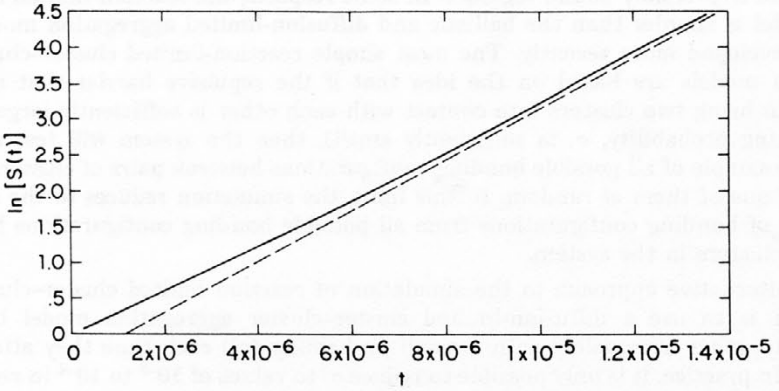

Figure 7. Time dependence of the mean cluster size obtained from three dimensional off-lattice simulations of reaction-limited cluster–cluster aggregation. These results were obtained from 123 simulations whit 200,000 particles in each simulation.

The kinetics of reaction-limited cluster–cluster aggregation can be simulated by increasing the time by a constant amount ($1/N_0^2$ is a convenient value) each time a pair of clusters is selected in the model described in the last part of the previous section. Figure 7 shows the time dependence of the mean cluster size obtained from three dimensional off-lattice simulations.

In practice, it is not easy to distinguish between power law growth (equation (23)) with a large value for the exponent z, exponential growth, or gelation [$S(t) \sim (t_g - t)^{-\theta}$] where t_g is a finite gel time. However, the results shown in Figure 7 do support the idea[65] that the mean cluster size grows exponentially.

Figure 8 shows the cluster size distribution obtained at 6 stages during similar off-lattice simulations. It appears that the cluster size distribution can be described as a power law with a cut off at large cluster sizes (equation (25)) with the exponent τ having a value of about 1.7.

The number of ways of combining clusters of size s_i and s_j is proportional to $s_i s_j$. However, many of these contacting configurations will involve overlap between the two clusters since $2D > d$. In this case, we expect that the elements of the reaction kernel $k(s_i,s_j)$ describing clusters of size s_i and s_j will have the form

$$K(s_i,s_j) \sim s_i s_j s_j^{(\lambda'-2)} \quad \text{for} \quad s_i \geq s_j \tag{70}$$

The quantity $s_j^{(\lambda'-2)}$ in equation (70) is a probability $P(s_j,s_j)$ that two clusters of size s_j brought into contact *via* randomly selected particles in each cluster will not overlap. The dependence of $P(s_j,s_i)$ on s_i is shown for both the lattice model and off-lattice model in Figure 9. The results in this figure indicate that the exponent λ' has a value of about 1.1 so that

$$K(s_i,s_j) \sim s_i^{\lambda} \tag{71}$$

where the exponent λ has a value of about 1.1 for both the lattice and off-lattice models.

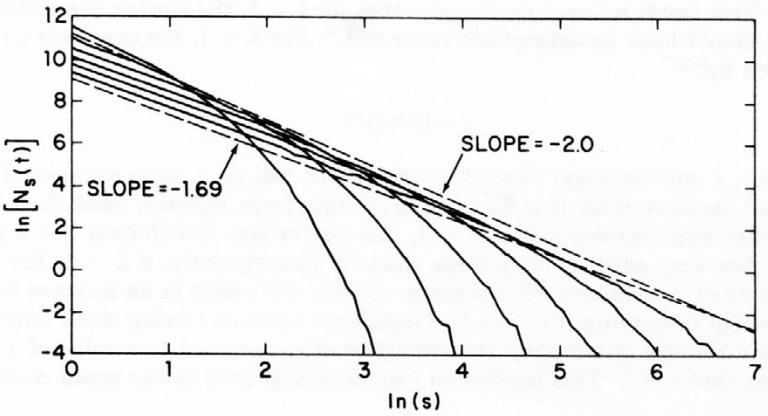

Figure 8. Cluster size distributions obtained at 6 stages (times) using a three dimensional off-lattice reaction-limited cluster–cluster aggregation model.

Ball *et al.*[65] have argued that the kernel model for three dimensional reaction limited cluster–cluster aggregation should have the form

$$k(s_i,s_j) \sim s_i s_j^{\lambda-1} \quad (s_i >> s_j) \tag{72}$$

and

$$k(s_i,s_j) \sim s_i^{\lambda} \quad (s_i \approx s_j) \tag{73}$$

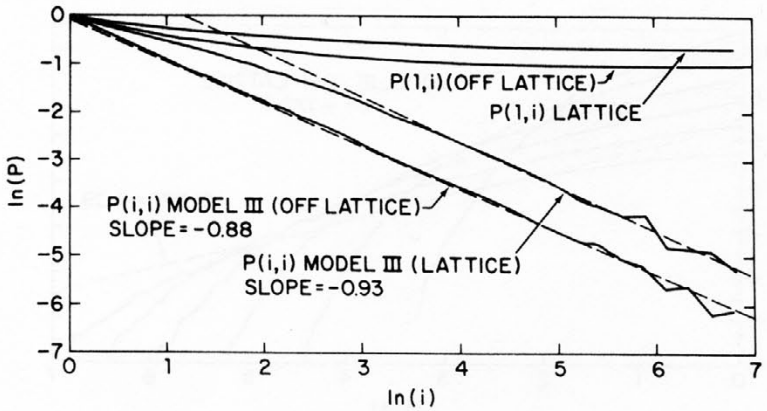

Figure 9. This figure shows the dependence of $P(i,i)$ and $P(1,j)$ on i for both the three dimensional off-lattice and the cubic lattice reaction-limited aggregation models. Here $P(i,j)$ is the probability that clusters containing i and j particles will not overlap after they have been brought into contact *via* a randomly selected pair of particles (one in each cluster).

with $\lambda = 1$. This result is based on the idea that for $\lambda = 1$, the cluster size distribution exponent τ should have an asymptotic value of 1.5. For $\lambda > 1$, the exponent τ rises to a value given by[66,67]

$$\tau = (3+\lambda)/2 \tag{74}$$

In this event, λ will be larger than 2 so that there will be a large number of single particles and small clusters that can penetrate into large clusters, raise their fractal dimensionality and decrease λ. For $\lambda < 1$, the cluster size distribution has a peaked shape with few very small or very large clusters. Consequently, if $\lambda < 1$, the fractal dimensionality of the clusters will decrease and this will result in an increase in λ. Because very small deviations of λ from the »singular« value of 1 bring about large changes in the cluster size distribution that would tend to restore λ to a value of 1.0. Ball *et al.* suggest that $\lambda = 1$. This implies an exponential growth in the mean cluster size

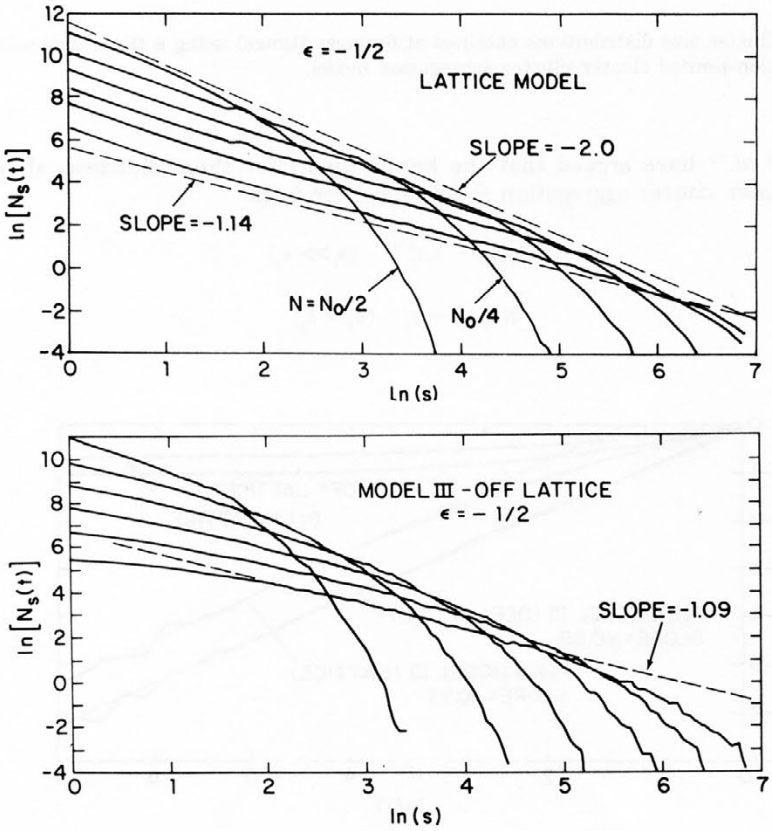

Figure 10. Time-dependent cluster-size distributions obtained from the lattice version (a, top) and off-lattice (b, bottom) of the reaction-limited cluster–cluster aggregation model with $\varepsilon = -1/2$. In each case, the curves correspond to cluster-size distributions obtained at the stage where the number of clusters had been reduced from an initial value of $N_0 = 200{,}000$ particles to $N_0/2$, $N_0/4 \cdots N_0/64$ ($N_0/2^n$, n = 1–6).

(in accord with both simulation results and experiments) and a value of 1.5 for the cluster size distribution exponent τ.

The source of the discrepancy between the theoretical results of Ball *et al.* and the simulation results (for the size distribution exponent, τ) is not well understood. The theoretical arguments are compelling but not rigorous. A more likely source of the discrepancy is a slow approach to the limiting asymptotic behavior in the simulations. A very slow approach to the asymptotic limit with »pseudo scaling« behavior at intermediate times is not at all uncommon.[68,69] Cluster size distribution exponents close to 1.5 have been found in a variety of experimental studies.[70-73] However, values for τ close to 2.0 have been found by Martin for the slow aggregation of colloidal silica.[74]

It is implicitly assumed in the simple reaction-limited cluster–cluster aggregation models described above that the rate at which bonding configurations are selected is proportional to their probability of being found in the system. It is possible that in real cluster–cluster aggregation (at least for reasonably small cluster sizes where translation is more important than internal modes), the rate at which two clusters join may depend on the frequency with which they »collide« as well as on the amount of time they spend together. It is also reasonable to suppose that the collision frequency for clusters i and j will be given by $\nu(i,j) \sim \mathcal{D}_i + \mathcal{D}_j$ when $\mathcal{D}_i$ and $\mathcal{D}_j$ are the cluster diffusion coefficients. Consequently, reaction limited aggregation models have been developed in which pairs of particles (i and j) are selected at random with probabilities $(s_i^{\varepsilon} + s_j^{\varepsilon})$ where s_i and s_j are the sizes of the clusters containing s_i and s_j particles, respectively. Figure 10 shows some of the results obtained from simulations carried out with $\varepsilon = -1/2$ (approximately $-1/D$) using both off-lattice and cubic lattice reaction-limited cluster–cluster aggregation models.

NONFRACTAL SYSTEMS

Although recent attention has been focussed primarily on aggregation processes leading to the formation of fractal structures, the general scaling approach emphasized in this chapter is also applicable to nonfractal systems. A scaling approach is valuable for many processes including spinodal decomposition,[75] droplet coalescence, and the aggregation of small particles to form compact ($D = d$) and linear ($D = 1$) structures.

Figure 11 and 12 show the results of three dimensional simulations of the diffusion-limited aggregation of oriented rods that can stick only at their ends.[76] Figures 11a and 11b show the algebraic time dependence of $S(t)$ and $N(t)$ obtained from simulations carried out with a diffusion coefficient exponent (γ) of -1. Here, it was assumed that, although the geometry of the rods is highly anisotropic, their diffusion is isotropic so that $\mathcal{D}_{||}(\zeta) = D_{\perp}(s) \sim s^{\gamma}$. In general, the exponents z and z' describing the time dependence of $N(t)$ and $S(t)$ are given by

$$z = z' = 1/(1 - \gamma) \tag{75}$$

This result is not surprising since only the ends of the rods are sticky and, at a sufficiently low concentration, this model becomes equivalent to the diffusion-limited particle coalescence model. In two dimensional simulations, we find that the decrease in the number of clusters or rods is given by equation (52) and

$$s(t) \sim [t/\ln(t)]^z \tag{76}$$

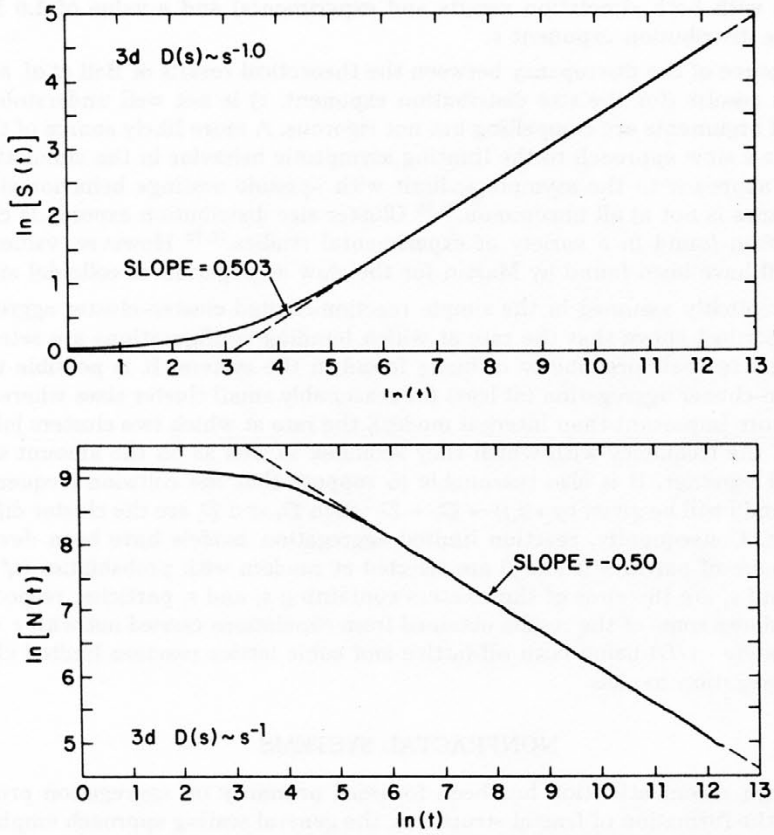

Figure 11. Time dependence of $S(t)$ (a, top) and $N(t)$ (b, bottom) obtained from a three dimensional (cubic lattice) model for the aggregation of oriented rods with size dependence diffusion coefficients given by equation (1) with $\gamma = -1$.

where z and z' are given by equation (75).

In one dimensional simulations the exponents z and z' are given by[76]

$$z = z' = 1/(2 - \gamma) \tag{77}$$

Figure 12 shows how the time dependent rod size distributions scale according to equation 2.

Another example is provided by the diffusion-limited droplet coalescence model.[77] In this model, hyperspherical D dimensional droplets follow random walk paths in a d dimensional box with periodic boundary conditions. Whenever two droplets with radii of R_1 and R_2 touch, they are coalesced to form a larger droplet with conservation of mass and the center of mass.

$$R = (R_1^D + R_2^D)^{1/D} \tag{78}$$

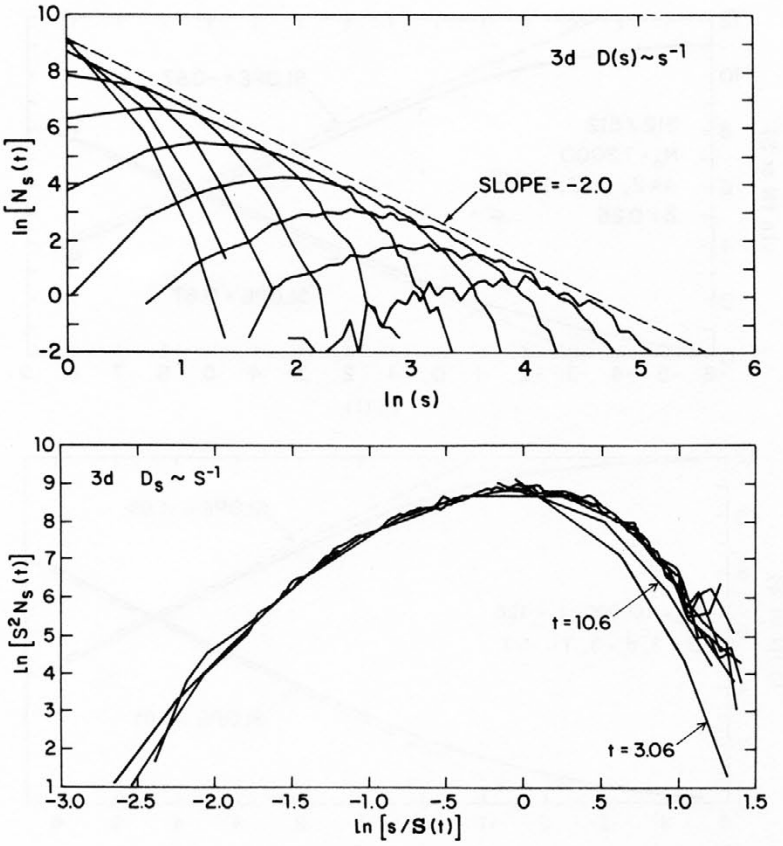

Figure 12. Scaling of the time dependent cluster size distributions ($N_s(t)$) for the simulations used to obtain Figure 11. Figure 12a (top) shows the cluster size distributions at ten different times and Figure 12b (bottom) shows how these size distributions can be scaled using the scaling form given in equation (2).

where R is the radius of the combined droplet and

$$\mathbf{X} = (s_1\mathbf{X}_1 + s_2\mathbf{X}_2)/(s_1 + s_2) \tag{79}$$

where $\mathbf{X}$, $\mathbf{X}_1$ and $\mathbf{X}_2$ are the coordinates of the combined droplet and the coalescing droplets. After coalescence, the environment of the coalesced droplet is examined for contact with other droplets and the coalescence process is continued until no further contacts are found. Figures 13a and 13b show the algebraic growth of S(t) and decays of N(t) for the cases $D = d = 2$, $\gamma = -1/D$ and $D = d = 3$, $\gamma = -1/D$. In this case, there are no logarithmic corrections in the two dimensional case since both the distance between droplets and their characteristic sizes (radii or diameters) grow in the same way.

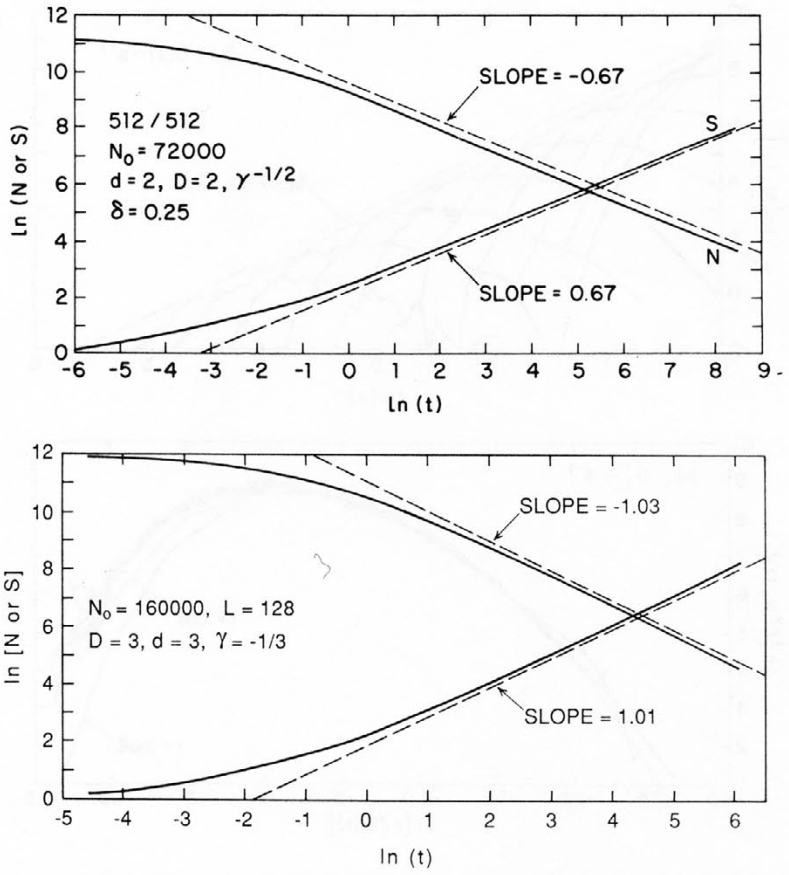

Figure 13. Time dependence of S and N obtained from diffusion-limited droplet coalescence models. Figure 13a (top) shows results from a simulation of the coalescence of two dimensional droplets in a two dimensional space with a diffusion coefficient exponent, γ, (equation (1)) of $-1/2$. Similarly, Figure 13b (bottom) shows results from a simulation carried out with $D = d = 3$ and $\gamma = -1/3$.

Consequently, the entire system can be rescaled at different times by a simple change of length scales. Figure 14 illustrates how the time dependent droplet size distribution can be scaled using the scaling form in equation (2) for the case $D = d = 2$, $\gamma = 0$. This scaling form is not restricted to the case $D = d$ and works well for all combinations of D, d and γ that result in power law growth of the mean droplet size.

In general, the time dependence of the number of droplets and the mean droplet size are given by equations (43) and (46) (with z given by equation (44)) for $d > 2$. For $d = 2$ and $D \neq 2$, logarithmic corrections appear in the time dependence of S and N. The exponents have the same dependence on D, d and γ as those associated with the diffusion-limited cluster–cluster aggregation model and the discussion of that model, given above, applies here also.

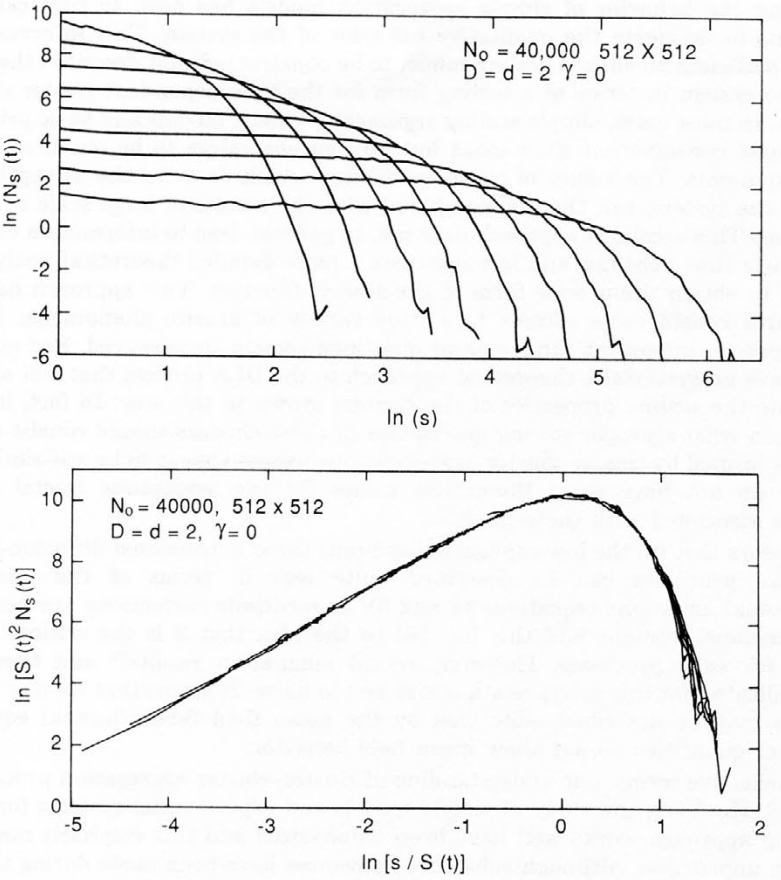

Figure 14. Time dependent droplet size distributions obtained from diffusion-limited droplet coalescence model simulations with $D = d = 2$ and $\gamma = 0$. Figure 14a (top) shows the droplet size distribution at nine times and Figure 14b (bottom) shows how these size distributions can be scaled using the scaling form given in equation (2).

SUMMARY

The aggregation of small particles to form large structures is important in many areas of science and technology. As a consequence, aggregation processes have been extensively studied throughout this century. During the past decade, the realization that a wide geometry of aggregation processes generate structures that have a fractal geometry and the availability of data from simple computer models has stimulated a renewed interest in the theoretical aspects of colloidal aggregation. Experimental studies and computer simulations have also strongly stimulated each other during this period.

In this survey I have emphasized the application of scaling ideas to the kinetics of aggregation processes. This is a very natural approach in the case of fractal aggregates but works equally well for non-fractal structures. A general approach to un-

derstanding the behavior of simple aggregation models has been to first carry out simulations to delineate the qualitative behavior of the system. This information is generally sufficient to allow a scaling model to be constructed that describes the evolution of the system in terms of a scaling form for the time dependent cluster size distributions. In most cases, simple scaling arguments, kinetic models and basic principles such as mass conservation allow exact but no rigorous values to be obtained for the scaling exponents. The values of these exponents, which describe the asymptotic behavior of the system, can then be compared with the results of large scale computer simulations. This »scaling« approach does not, in general, lead to information concerning the early time behavior and in most cases a more detailed theoretical analysis[77-79] is needed to obtain the precise form of the scaling function. This approach has been applied with considerable success to a wide variety of kinetic phenomena. Despite these successes, important fundamental questions remain unanswered. For example, we still have no systematic theoretical approach to the DLA process that will allow us to calculate the scaling properties of the clusters grown in this way. In fact, it is not even certain what a proper scaling description of these clusters should consist of. The structures formed by cluster–cluster aggregation processes appear to be self-similar but again we do not have exact theoretical values for the asymptotic fractal dimensionalities associated with these models.

It appears that (in the low concentration limit) three dimensional diffusion-limited aggregation processes can be described quite well in terms of the »classical« Smoluchowski equations (equations (4 and 5). Logarithmic corrections are needed in tow dimensional systems and this has led to the idea that 2 is the critical dimensionality for such processes. However, recent simulation results[80] and theoretical ideas[81] indicate that this interpretation may be too naive. It seems that for $d = 3$ some quantities may be described quite well by the mean field Smoluchowski equations while other quantities do not show mean field behavior.

In qualitative terms, our understanding of cluster–cluster aggregation processes is quite good. However, the study of simple models and experimental systems for which the scaling approach works well have been emphasized and this emphasis may leave the wrong impression. Although substantial advances have been made during the past decade, much work remains to be done. We know little about the kinetics of aggregation in concentrated systems that are of considerable practical importance. Another area of considerable importance that has only just begun to be investigated is the deposition of fractal aggregates onto surfaces and their subsequent compactification. Such phenomena are important in commercial processes and in areas such as geophysics. Similarly, processes such as the sintering of fractal aggregates and their restructuring *via* processes such as »ripening« and diagenesis have not yet been extensively explored.

A variety of experimental systems has been found that come close to realizing the conditions associated with simple models such as DLA, cluster–cluster aggregation models and droplet coalescence models. However, most experimental systems are quite complicated and for this reason experiments are not generally the best way of testing theoretical ideas. The results of experimental studies are of course the motivation for all of the work described in this survey. The simple models which are the main subject of this survey provide a foundation for the development of more complex models that better describe the behavior of real systems. Some progress has been made in this direction, but a systematic study of the kinetics associated with these models is for the most part absent and I am aware of no serious attempts to compare the results of simulations and experimental studies for these, more complex, models.

Acknowledgement. – My interest in aggregation and fractals has been stimulated by valuable interactions with many colleagues and collaborators. I would like to acknowledge the contributions of those including R. C. Ball, Z. Y. Chen, J. M. Deutch, Z. Djeordjević, D. Donn, M. H. Ernst, F. Family, K. Kang, R. Klein, F. Leyvraz, M. Y. Lin, H. M. Lindsay, E. D. McGrady, G. W. Mulholland, S. Redner, T. Vicsek, D. A. Weitz and R. M. Ziff with whom I have collaborated on various projects in the area of aggregation kinetics.

REFERENCES

1. B. B. Mandelbrot, *The Fractal Geometry of Nature,* W. H. Freeman and Company, New York 1982.
2. T. A. Witten and L. M. Sander, *Phys. Rev. Lett.* **47** (1981) 1400.
3. P. Meakin in *Phase Transitions and Critical Phenomena*, Vol. 12. C. Domb and J. L. Lebowitz, eds., Academic Press, 1988, p. 335.
4. R. C. Ball in *On Growth and Form: Fractal and Non-Fractal Patterns in Physics*, NATO ASI Series E100. H. E. Stanley and N. Ostrowsky, eds., Martinus Nijhoff, Dordrecht, 1986, p. 69.
5. M. Matsushita in *The Fractal Approach to Heterogeneous Chemistry: Surfaces, Colloids and Polymers*, D. Avnir, ed., Wiley, Chichester, 1989.
6. P. Meakin, *Phys. Rev. Lett.* **51** (1983) 1119.
7. M. Kolb, R. Botet, and R. Jullien, *Phys. Rev. Lett.* **51** (1983) 1123.
8. D. A. Weitz and M. Oliveria, *Phys. Rev. Lett.* **52** (1984) 1433.
9. R. Botet, *J. Phys.* **A18** (1985) 847.
10. D. N. Sutherland, *J. Colloid Interface Sci.* **25** (1967) 373.
11. D. N. Sutherland, Nature **226** (1970) 1241.
12. D. N. Sutherland and I. Goodarz-Nia, *Chem. Eng. Sci.* **26** (1971) 2071.
13. J. H. Jeans, *The Dynamic Theory of Gases*, Dover, New York, 1954.
14. P. Meakin and B. Donn, *Astrophys. J.* **329** (1988) L39.
15. R. Jullien and M. Kolb, *J. Phys.* **A17** (1984) L639.
16. M. Kolb and R. Jullien, *J. Physique Lett.* **46** (1984) L977.
17. M. Y. Lin, H. M. Lindsay, D. A. Weitz, R. C. Ball, R. Klein, and P. Meakin, *Phys. Rev.* **A41** (1990) 2005.
18. T. Vicsek and F. Family, *Phys. Rev. Lett.* **52** (1984) 1669.
19. R. Botet and R. Jullien, *J. Phys.* **A17** (1984) 2517.
20. M. Kolb, *Phys. Rev. Lett.* **53** (1984) 1653.
21. P, Meakin, T. Vicsek, and F. Family, *Phys. Rev.* **B31** (1985) 564.
22. M. V. Berry and I. C. Percival, *Opt. Acta* **33** (1986) 577.
23. J. Frey, J. J. Pinvidii, R. Botet, and R. Jullien, *J. Phys. (France)* **49** (1988) 1969.
24. J. Nelson, *Nature* **339** (1989) 611.
25. Z. Chen, P. Sheng, D. A. Weitz, H. M. Lindsay, M. Y. Lin, and P. Meakin, *Phys. Rev.* **B37** (1988) 5232.
26. Z. Y. Chen, P. Weakliem, W. M. Gelbart, and P. Meakin, *Phys. Rev. Lett.* **58** (1987) 1996.
27. P. Meakin, B. Donn, and G. W. Mulholland, *Langmuir* **5** (1989) 510.
28. Z. Y. Chen, J. M. Deutch, and P. Meakin, *J. Chem. Phys.* **80** (1984) 2982.
29. P. Meakin, Z. Y. Chen, and J. M. Deutch, *J. Chem. Phys.* **82** (1985) 3786.
30. W. Hess, H. L. Frisch, and R. Klein, *Z. Phys.* **B64** (1986) 65.
31. W. Van Sarloos, *Physica* **147A** (1987) 280.
32. P. Wiltzius, *Phys. Rev. Lett.* **58** (1987) 710.
33. Z. Y. Chen, P. Meakin, and J. M. Deutch, *Phys. Rev. Lett.* **59** (1987) 2121.
34. P. N. Pusey, J. G. Rarity, R. Klein, and D. A. Weitz, *Phys. Rev. Lett.* **59** (1987) 2122.
35. P. Wiltzius and W. Van Sarloos, *Phys. Rev. Lett.* **59** (1987) 2123.
36. Y. Kantor and T. A. Witten, *J. Phys. Lett. (France),* **45** (1984) L675.
37. Y. Kantor and I. Webman, *Phys. Rev. Lett.* **52** (1984) 216.
38. G. Deutscher, R. Maynard, and O. Parodi, *Europhys. Lett.* **6** (1988) 49.
39. R. Buscall, P. D. A. Mills, J. W. Goodwin, and D. W. Lawson, *J. Chem. Soc. Faraday* **84** (1988).
40. J. Forsman, J. P. Harrison, and A. Rutenberg, *Can. J. Phys.* **65** (1987) 767.

41. T. Woignier, J. Phalippou, R. Sempere, and J. Pelous, *P. Phys. (France)* **49** (1988) 289.
42. S. Alexander and R. Orbach, *J. Phys. Lett. (France)* **43** (1982) L625.
43. Y. Gefen, A. Aharony, and S. Alexander, *Phys. Rev. Lett.* **50** (1983) 77.
44. S. Havlin and D. Ben Avraham, *Adv. Phys.* **36** (1987) 695.
45. R. Rammal and G. Toulouse, *J. Phys. Lett. (France)* **44** (1983) L13.
46. P. Meakin and H. E. Stanley, *Phys. Rev. Lett.* **51** (1983) 1457.
47. A. Aharony and J. Feder, eds., *Fractal in Physics: Essays in Honor of Bennoit B. Mandelbrot*, North Holland, Amsterdam, 1989.
48. M. von Smoluchowski, *Z. Phys.* **17** (1916) 585.
49. M. von Smoluchowski, *Z. Phys. Chem.* **92** (1917) 129.
50. A. A. Lushnikov, *J. Colloid Interface Sci.* **45** (1973) 549.
51. R. L. Drake in *Topics in Current Aerosol Research, Part 2. International Reviews in Aerosol Physics and Chemistry*, Vol. 3. G. M. Hidy and J. R. Brock, eds., Pergamon, New York, 1972.
52. S. K. Friedlander, *Smoke, Dust and Haze*, Wiley, New York, 1977.
53. S. K. Friedlander and C. S. Wang, *J. Colloid Interface Sci.* **22** (1966) 126.
54. R. Jullien and R. Botet, *Aggregation and Fractal Aggregates*, World Scientific, Singapore, 1987.
55. T. Vicsek, *Fractal Growth Phenomena*, World Scientific, Singapore, 1989.
56. P. Meakin, *Adv. Colloid Interface Sci.* **28** (1988) 249.
57. P. Meakin, unpublished.
58. K. Kang and S. Redner, *Phys. Rev.* **A30** (1984) 2833.
59. R. M. Ziff, E. D. McGrady, and P. Meakin, *J. Chem. Phys.* **82** (1985) 5269.
60. P. Meakin, *Ann. Rev. Phys. Chem.* **39** (1988) 237.
61. P. Meakin and F. Family, *Phys. Rev.* **A36** (1987) 5498.
62. W. D. Brown and R. C. Ball, *J. Phys.* **A18** (1985) L527.
63. F. Leyvraz, preprint.
64. P. Meakin and F. Family, *Phys. Rev.* **A38** (1988) 2110.
65. R. C. Ball, D. A. Weitz, T. A. Witten, and F. Leyvraz, *Phys. Rev. Lett.* **58** (1987) 274.
66. P. G. J. Van Dongen and M. H. Ernst, *Phys. Rev. Lett.* **54** (1985) 1396.
67. P. G. J. Van Dongen and M. H. Ernst, *J. Phys.* **A18** (1985) 2779.
68. K. Kang, S. Redner, P. Meakin, and F. Leyvraz, *Phys. Rev.* **A33** (1986) 1171.
69. T. W. Taylor and C. M. Sorensen, *Phys. Rev.* **A36** (1987) 5415.
70. C. K. Von Schulthess, G. B. Benedek, and R. W. de Blois, *Macromolecules* **13** (1980) 939.
71. D. A. Weitz, J. S. Huang, M. Y. Lin, and J. Sung, *Phys. Rev. Lett.* **54** (1985) 1416.
72. M. L. Broide, *Experimental Study of Aggregation Kinetics: Dynamic Scaling of Measured Cluster-Size Distributions*, Thesis, Massachusetts, Institute of Technology, 1988.
73. J. G. Rarity, R. S. Seabrook, and R. G. Carr, *Proc. Roy. Soc., London* **A423** (1989) 89.
74. J. E. Martin, *Phys. Rev.* **A36** (1987) 3415.
75. J. D. Gunton, M. San Miguel, and P. S. Sahni in: *Phase Transitions and Critical Phenomena*, C. Domb and J. L. Lebowitz, eds., Academic, London Vol. 8 (1983) p. 267.
76. S. Miyazima, P. Meakin, and F. Family, *Phys. Rev.* **A36** (1987) 1421.
76a. P. Meakin, *Physica* **165** (1990) 1.
77. M. H. Ernst, R. M. Ziff, and E. M. Hendriks, *J. Colloid Interface Sci.* **97** (1984) 266.
78. E. M. Hendriks and M. H. Ernst, *J. Colloid Interface Sci.* **97** (1984) 176.
79. F. Leyvraz and H. R. Tschudi, *J. Phys.* **A14** (1981) 3389.
80. P. Meakin and M. H. Ernst, *Phys. Rev. Lett.* **60** (1988) 2503.
81. P. G. J. Van Dongen, *Phys. Rev. Lett.* **63** (1989) 1281.

SAŽETAK

Simulacija kinetike agregacije: fraktali i skaliranje

P. Meakin

U mnogim procesima od interesa za fiziku, kemiju i biologiju, male čestice se udružuju i stvaraju veće strukture. Fraktalna geometrija agregata malih čestica igra važnu ulogu u njihovom fizičkom ponašanju, uključujući i samu kinetiku agregacije. Kinetika agregacije često se može opisati pomoću jednadžbe prosječnog polja Smoluchowskoga. Geometrijska svojstva mjerne skale (fraktalna geometrija) agregirajućih nakupina (cluster) određuju skalnu simetriju reakcijske jezgre, koja pak određuje asimptotski oblik raspodjele veličine nakupina. U najjednostavnijim sustavima asimptotska raspodjela veličine nakupina može se opisati pomoću skalnog oblika $N_s(t) \sim s^{-\theta} f(s/S(t))$, gdje je $N_s(t)$ broj nakupina veličine s u vremenu t, a $S(t)$ je prosječna veličina nakupina u vremenu t. Oblik skaliranja može se upotrijebiti u uvjetima, kada jednadžba Smoluchowskoga ne osigurava odgovarajući prikaz kinetike agregacije.